Dipole nanoantennas of single-walled carbon nanotube bundles: A numerical analysis

Ángel Salazar[1], F. R. Pérez[1] and Álvaro Ospina-Sanjuan[2]

[1]Grupo de Óptica y Espectroscopía (GOE), Centro de Ciencia Básica, Universidad Pontificia Bolivariana, Cq. 1 # 70-01, Medellín, Colombia.
[2]Grupo de Investigación en Bioingeniería y Microelectrónica, Facultad de Ingeniería Eléctrica y Electrónica, Universidad Pontificia Bolivariana, Cq. 1 # 70-01, Medellín, Colombia.

Corresponding author: Ángel Salazar (e-mail: angel.salazar@upb.edu.co).

ABSTRACT Carbon nanotube-based nanoantennas could configure important components in devices for applications in various fields, such as sensing, imaging, and signal transmission at the nanoscale. One of the factors that can affect the properties and, therefore, the performance of the nanoantenna is the temperature. In this work, the resonance properties at different temperatures for dipole nanoantennas formed from bundles of densely packed carbon nanotubes are analyzed. Calculations are made from the Hallén equation using the dynamic quantum conductivity and an equivalent radius for the antenna based on the surface area of the bundle. Results are obtained in the range from 1 GHz to1000 GHz and temperatures from 200K to 500K. A detailed calculation of the relaxation frequency is performed to consider the possible interaction of electrons with defects and acoustic and optical phonons. Input impedance, first resonance frequency, and radiation efficiency are obtained for different numbers of nanotubes in the bundle. Results show a significant effect of the temperature and surface area of the bundle on these parameters.

INDEX TERMS Carbon nanotube, Hallen's equation, Input impedance, Nanoantenna.

I. INTRODUCTION

CARBON nanotubes (CNT) have shown interesting properties for industrial, biomedical, interconnects, photonics, and a diversity of applications in nanotechnology [1],[2]. In particular, metallic single-walled carbon nanotubes (SWCNT) have been studied in configurations for nanoantennas [3]-[5]. One of the most interesting aspects is that CNT-based nanoantenas and devices could perform in the gap of THz, a narrow band of the electromagnetic spectrum between microwaves and infrared (0.1-10 THz) that has been underutilized in some way. On the one hand, devices for the transmission and reception of data in this gap need to be miniaturized due to the shorter wavelength of the radiation. On the other hand, the emission in THz is not common in materials. In this sense, nanomaterials such as graphene and carbon nanotubes, with their low dimensionality and outstanding conductive properties, provide a great possibility for the design of devices that work in this range [6]-[8]. Quantum or semiclassical physical models should be used to describe the physics of such devices. Now, one of the difficulties against SWCNT antennas is their low efficiency. Because of the small radius of the nanotube, a large impedance is present that strongly reduces the radiation efficiency [9], [10]. Nevertheless, these types of nanoantennas could also be properly integrated into high impedance nanoelectronic circuits, which are very sensitive to extremely low currents in such a way that the low efficiency of the antenna, at least in principle, would not constitute a serious problem for the detection of the signals. Even so, some research efforts have been focused on SWCNT bundles and other structures of CNT antennas with which the possibility of overcoming the problem of low efficiency has been visualized [11]-[18]. In particular, in [11], for example, an electromagnetic modeling approach of bundles of SWCNT with circular geometry for dipole antenna applications was reported. In this reference, a single solid equivalent material to model the CNT and the bundle of nanotubes is considered to use the CST (MWS) software package. Similar work was done in [12] for bundles with rectangular cross-sections. Commonly, the relaxation frequency of the nanotube is taken as a phenomenological relaxation frequency, which is appropriate for acoustic phonons, and the analysis is done at room temperature. In general, published works on CNT-based nanoantennas use typical values of the relaxation time at room temperature. An interesting discussion related to the values for the relaxation time at low and optical frequencies at room temperature was presented in [9]. Later, in [19], an approximated model was used to calculate the effective mean free path as a function of temperature and relaxation frequency to analyze the scattering properties of isolated CNTs and CNT arrays. That approximated model was based on the study about the electrical and thermal transport in metallic single-wall carbon nanotubes reported in [20]. It was found that, since the temperature affects the mean free path, thus affecting the resistance of the nanotube, and since the capacitance and

inductance are not affected, the resonance frequencies were stable while the peaks decreased in amplitude as temperature increased. In [19], calculations were presented for relatively low temperature increases relative to room temperature, for 300 and 320 K. Now, since temperature is expected to have a significant effect on the performance of a nanoantenna, in this work, we focus on dipole nanoantennas of SWCNT bundles and, using a simplified model based on the effective surface area of the bundle, their resonances properties are analyzed. The motivation that guides the work is that carbon nanotube bundles offer high aspect ratios, and tunable electronic properties, which would lead to enhanced antenna performance in terms of impedance matching, current distribution, and radiation efficiency. Results are obtained for different temperatures from 200 to 500 K and in the range of 1 GHz up to 1 THz, thus covering a portion of the terahertz gap. A detailed calculation of the relaxation frequency is performed to consider the possible interaction of electrons with defects and acoustic and optical phonons. Input impedance and radiation efficiency results are obtained for different numbers of nanotubes in the bundle. The paper is organized as follows. In Section 2, the most relevant aspects of the theoretical model are discussed. Section 3 gives a brief description of the numerical procedure, and in Section 4, results are presented and analyzed. Conclusions are presented in Section 5.

II. THE HALLÉN'S INTEGRAL EQUATION

Let us consider a dipole nanoantenna whose arms are metallic CNTs (Fig. 1). The current on the surface can be obtained by Hallen's integral equation [5], [9], [10]. This equation results from the relation between the electric field $\vec{E}$ and the magnetic vector potential $\vec{A}$,

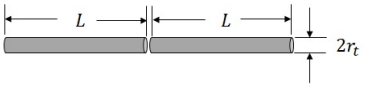

FIGURE 1. A scheme of a CNT dipole antenna.

$$\vec{E}(\vec{r}) = -j\omega\left(1+\frac{1}{k^2}\vec{\nabla}\vec{\nabla}\cdot\right)\vec{A}(\vec{r}) \tag{1}$$

$$\vec{A}(\vec{r}) = \frac{\mu}{4\pi}\int_V \vec{J}(\vec{r})\frac{e^{-jk|\vec{r}-\vec{r}'|}}{|\vec{r}-\vec{r}'|}d\vec{r}' \tag{2}$$

$\vec{J}(\vec{r})$ is the current density, ω is the angular frequency of the fields, and k is the wavenumber. For a thin wire oriented along the z direction and with a radius r_t much smaller than its length $2L$ and the wavelength λ of the fields, the current can be considered filamentary. The current density would be given by,

$$J_z(z) = \frac{I(z)}{2\pi r_t} \tag{3}$$

Besides, (1) is reduced in this case to,

$$E_z = -j\omega\left(1+\frac{1}{k^2}\frac{\partial^2}{\partial z^2}\right)A_z \tag{4}$$

and the magnetic potential is given by,

$$A_z(z) = \frac{\mu}{4\pi}\int_{-L}^{L} I(z')K(z-z')dz' \tag{5}$$

$K(z-z')$ is the kernel given in approximate form by,

$$K(z-z') = \frac{e^{-jk\sqrt{(z-z')^2+r_t^2}}}{\sqrt{(z-z')^2+r_t^2}} \tag{6}$$

Now well, the current density is also given by,

$$J_z(z) = \sigma[E_z^s(z) + E_z^i(z)] \tag{7}$$

where σ is the conductivity, $E_z^i(z)$ is the incident or impressed electric field on the antenna, and $E_z^s(z)$ is the scattered electric field. Equating (3) and (7), the scattered field is,

$$E_z^s(z) = \frac{I(z)}{2\pi r_t\sigma} - E_z^i(z) \tag{8}$$

Thinking of the electric field E_z in (4) as the scattered electric field, assuming that the impressed electric field E_z^i is produced by a delta-gap voltage source centered in the origin, $E_z^i(z') = V_{in}\delta(z')$ [21], defining the impedance per unit length as,

$$z_i = \frac{1}{2\pi r_t\sigma} \tag{9}$$

replacing (8) and (5) in (4), and using the Green's Method, the Hallén's equation is obtained,

$$\int_{-L}^{L}[K(z-z') + q(z-z')]I(z')dz' = d_1 sin(kz) + d_2 cos(kz) - j\frac{4\pi\omega\varepsilon V_{in}}{2k}sin(k|z|) \tag{10}$$

with

$$q(z-z') = \frac{\omega\varepsilon}{r_t\sigma}\frac{e^{-jk|z-z'|}}{k} \tag{11}$$

In this integral equation, $\boldsymbol{I(z')}$ is then the current on the antenna to be determined, $\boldsymbol{z'}$ is the coordinate of a source point on the antenna axis, and $\boldsymbol{z}$ is the coordinate of the field point. $\boldsymbol{d_1}$ and $\boldsymbol{d_2}$ are constants to be determined in the solution process of the equation as well.

III. DIPOLE NANOANTENNAS OF SINGLE-WALLED CARBON NANOTUBE BUNDLES

In the definition of z_i in (9), $2\pi r_t$ is the perimeter of the circumference of the antenna. If each arm of the antenna is a SWCNT, $r_t = a$ is the radius of the nanotube, and the surface area is $2\pi aL$, where L is the nanotube length. If each arm of the nanoantenna is a bundle of identical SWCNTs, following

[22], the surface area of a bundle made with only two identical SWCTs is twice the area of each one of the individual SWCNTs, that is, $2(2\pi aL)$. If the bundle is formed with three SWCNTs, the surface area is 2.5 times the surface area of one of the nanotubes, that is, $2.5(2\pi aL)$. Each SWCNT added to the bundle produces an increase in the surface area of the bundle equals to 0.5 times the surface area of one of the SWCNTs. This sequence is valid up to a total of six SWCNT in the bundle, and in this case, the surface area is 4 times the surface area of a nanotube. If the bundle has seven densely packed SWCNTs, a first layer is completed, and the surface area is again 4 times the surface area of a nanotube, as can be deduced from Fig. 2. Therefore, in principle, it would be possible to replace the surface area of a bundle of N densely packed identical nanotubes by the surface area of an equivalent tube of radius la, that is, $2\pi(la)L$, where $l = 1, 2, 2.5, 3, 3.5, 4, 4$ (Fig. 3). Similar reasoning can be done to find the equivalent surface area if more nanotubes are added to the beam.

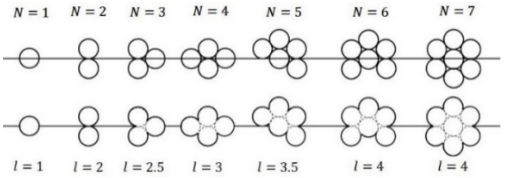

FIGURE 2. Construction of a bundle by joining 2, 3, 4, 5, 6 and 7 SWCNTs.

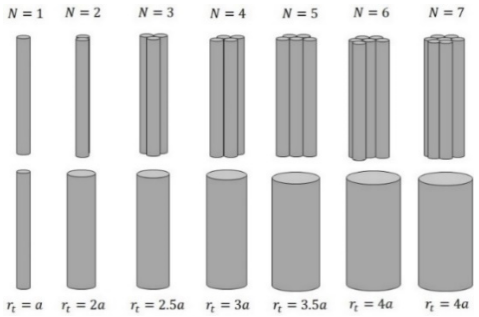

FIGURE 3. The sequence of tubes with a surface area equivalent to the surface area of a bundle of SWCNTs.

Considering the reasoning above with $r_t = la$ and, as in [15], that only the outermost nanotubes in the bundle contribute to the far-zone radiation, and the radiation of the inner nanotubes is shielded by the outer nanotubes, dipole nanoantennas of densely packed single-walled carbon nanotube bundles can be modeled as dipole antennas whose radii are a multiple of the radius of the SWCNTs from which they are built. Although this assumption seems plausible, experiments should be conducted to test the predicted behavior. To solve the Hallen's equation in (10), the conductivity σ must be replaced by the conductivity of CNTs. The dynamic two-dimensional surface conductivity for SWCNTs was obtained in [23] and, for small radius armchair CNTs, in the low frequency, GHz and lower THz, where interband transitions are not significant, it is given by,

$$\sigma_{cn}(\omega) \cong -j\frac{2e^2 \mathrm{v}_F}{\pi^2 \hbar a(\omega - j\nu)} \tag{12}$$

Armchair SWCNTs present a metallic behavior without an energy bandgap. In (12), j is the imaginary unit, a is the radius of the CNT, which, for metallic CNTs, is given by $a = 3bm/2\pi$, where $b = 0.142$ nm is the distance between nearest neighbor atoms in graphene and m is an integer greater than zero, e is the electron charge, v_F is the Fermi speed, which is of the order of 10^6 m/s, $\hbar$ is the reduced Planck's constant, ω is the electric field angular frequency, $\nu = 1/\tau$ is the relaxation frequency which accounts for the number of scattering events per second of the electrons, and τ is the relaxation time. The relaxation frequency depends on the interaction of electrons with defects and acoustic and optical phonons in the nanotubes and can be calculated using the Matthiessen formula [20], [24]. The current I on the antenna as a function of the frequency of the scattered electric field can be obtained by using (12) in (11) and then numerically solving (10) by the method of moments (MOM) [5], [25]. It was shown in [26] that if the numbers of subintervales N into which the antenna is divided is such that $N \gg L/a$ and the approximate kernel is used for calculations, oscillations appear in the obtained current at the ends and center of the antenna. Therefore, using the exact kernel is necessary in this case. Specific studies for carbon nanotube nanoantennas were first reported in [27]. Taking this into account, in the present and in our previous work [5], calculations were performed with $N = 1000$, so that the number of subintervals was much lower than the ratio L/a in all the considered cases, and the approximate kernel was used. After that, the input impedance can be obtained as $Z_{in} = V_{in}/I(0)$, where $I(0)$ is the current at the center of the antenna. The radiation efficiency can be calculated according to [28],

$$\eta = \frac{R_{in}}{R_{in}+R_{hf}}; \quad R_{hf} = \Re\left\{\frac{2L}{2\pi(la)}\sqrt{\frac{\omega\mu_o}{2\sigma}}\right\}; \quad R_{in} = \Re\{Z_{in}\} \tag{13}$$

where $\Re\{\cdots\}$ stands for the real part.

IV. EFFECTIVE MEAN FREE LENGTH OF SWCNTs

The effective mean free length $l_{m,eff}$ for the electrons in SWCNTs can be calculated by the Matthiessen formula [20], [24],

$$\frac{1}{l_{m,eff}} = \frac{1}{l_{ac}} + \frac{1}{l_{op}} + \frac{1}{l_d} \tag{14}$$

l_d is the mean free length considering possible defects in the CNT. It is expected that the density of defects increases with the CNT radius, but it seems to be a weak dependence. Moreover, the defect density does not increase with the temperature. Therefore, l_d can be considered a constant quantity. On the other hand, the mean free length l_{ac} for the electron due to the interaction with acoustic phonons is given by,

$$l_{ac} = \alpha_{ac}\frac{2a}{T} = l_{ac,300}\frac{T_{300}}{T} \quad (15)$$

where T is the absolute temperature, α_{ac} is a parameter in the range from 4.00×10^5 to 5.65×10^5K [5], $T_{300} = 300$K, and $l_{ac,300}$ is the room free mean length for the CNT of interest. If a (40,40) CNT is assumed, then its radius is $a = 2.713$ nm. Taking $\alpha_{ac} = 4.00 \times 10^5$K and $T = 300$K, then, from (15), a value of 7.233μm is obtained for $l_{ac,300}$, which is used in our calculations. If only optical phonons were considered, the mean free length l_{op}would have two contributions and is given by,

$$\frac{1}{l_{op}} = \frac{1}{l_{op,abs}} + \frac{1}{l_{op,ems}} \quad (16)$$

where, $l_{op,abs}$ is the mean free length considering the absorption of optical phonons by the electron and is given by,

$$l_{op,abs} = l_{op,300}\frac{N_{op}(T_{300})+1}{N_{op}(T)} \quad (17)$$

where,

$$N_{op}(T) = \frac{1}{\exp(E_{op}/k_BT)-1} \quad (18)$$

$k_B = 1.381x10^{-23}$ J/K $= 8.625x10^{-5}$ eV/K is the Boltzmann constant. E_{op} has been currently used as a fitting parameter for experimental data on electric transport in metallic CNT with values between 0.15-0.2 eV. We took $E_{op} = 0.16$eV for our numerical calculations, which has been a successful value in explaining experimental results related to electron transport in metallic CNTs [24].

On the other side, $l_{op,ems}$ is the mean free length considering the emission of optical phonons, which, at the same time, has two contributions and is given by,

$$\frac{1}{l_{op,ems}} = \frac{1}{l_{ems,E}} + \frac{1}{l_{ems,abs}} \quad (19)$$

$l_{ems,E}$ is the mean free length that results from the emission of an optical phonon by the electron after it has gained sufficient energy from the applied electric field and is given by,

$$l_{ems,E}(T) = \frac{E_{op}}{eE} + l_{op,300}\frac{N_{op}(T_{300})+1}{N_{op}(T)+1} \quad (20)$$

where E is the magnitude of the electric field and $l_{op,300}$ would be the scattering length for the CNT at room temperature, however, it is considered another fitting parameter that is usually taken between 10-100 nm. We assume $l_{op,300} = 100$nm.

$l_{ems,abs}$ is the mean free length that results because an electron can absorb an optical phonon and, after a distance, re-emit this phonon and is given by,

$$l_{ems,abs}(T) = l_{op,abs}(T) + l_{op,300}\frac{N_{op}(T_{300})+1}{N_{op}(T)+1} \quad (21)$$

For the $l_{m,eff}$ calculation, a value of $l_d = 8\mu$m is assumed. A low applied electric field $E = 4$ mV/μm was also assumed for the l_{op} calculations.

V. RESULTS AND DISCUSSION

We calculated the current distribution and input impedance for dipole nanoantennas of densely packed SWCNT bundles, by solving (10) numerically in the range from 1GHZ to 1000GHz. At temperatures lower than room temperature, the dispersion by acoustic phonons is the dominant scattering mechanism under low-field and low-frequency conditions. Temperatures higher than room temperature could cause scattering of the electrons by optical phonons, which would result in a very short electron mean free path and, hence, a high relaxation frequency. A high-applied electric field also contributes to activate optical phonons reducing even more the effective mean free path. To analyze only the temperature effect and do the calculations conceptually consistent with a low applied electric field, the input voltage was taken as $V_{in} = 4$ mV. An armchair SWCNT with $m = 40$ ($a = 2.712$ nm) is considered, and resonance properties of dipole nanoantennas built with bundles of this nanotube are explored at $T = 200$K, 300K, 400K, and 500K. At these temperatures, assuming the possibility of scattering by defects and acoustic and optical phonons, the respective effective mean free lengths, $l_{m,eff}$ are, 4.10 μm, 3.04 μm, 1.89 μm, and 1.14 μm. Therefore, from $l_{m,eff} = \mathrm{v_F}\tau = \mathrm{v_F}/\nu$, and taking the Fermi speed $\mathrm{v_F} = 10^6$ m/s, the corresponding relaxation times are 4.10 ps, 3.04 ps, 1.89 ps and 1.14 ps, and the respective relaxation frequencies are, $\nu = 2.44 \times 10^{11}\mathrm{s}^{-1}$, $3.29 \times 10^{11}\mathrm{s}^{-1}$, 5.29×10^{11} s^{-1} and 8.77×10^{11} s^{-1}. In the following, results for a nanoantenna with a total length of $2L = 20$ μm are presented. Notice that the total length is larger than the mean free path in any of the cases such that the model is adjusted to a situation without ballistic conduction. Now, well, it is know that current in dipole nanoantennas based on CNT is strongly attenuated for frequencies higher than $F_v = \mathrm{v}_F/2\pi a$ [9], [10]. For $a = 2.712$ nm, $F_v \approx 56$THz. Therefore, considering that infrared frequencies are in the range 300 GHz-430 THz, approximately, then, calculations below are done up to 1 THz frequencies, where (12) is reliable, without considering the optical range. Table 1 contains results about the first resonant frequency and the corresponding input impedance obtained for the nanoantennas at the different temperatures considered. The input impedance has been normalized by the quantum resistance of metallic CNTs $R_q = 6.45$ kΩ [24]. A comparison, including the results for the radiation efficiency, is presented between the simple nanoantenna built with arms

of only one SWCNTs and nanoantennas with arms consisting of 1- and 2-layer nanotube bundles.

TABLE 1. Values of the first resonance frequency and normalized input impedance at different temperatures for SWCNT bundle dipole nanoantennas with a total length of $2L = 20$ μm.

$2L = 20$ μm, $m = 40$ ($r_t = 2.712$ nm), Range: 1-1000 GHz							
l	T (K)	Relaxation time $\tau = l_{m,eff}/v_F$ (ps)	First resonant frequency (GHz)	Input impedance Z_{in} (Ω)	Modulus of the normalized input impedance $\lvert Z_{in}\rvert/R_0$	Efficiency	$F_v = v/2\pi$ (GHz)
1	200	4.10	161.45	8083.6-0.74948i	1.25	0.0024	38.8
	300	3.04	162.73	10944-1.5664i	1.70	0.0027	52.4
	400	1.89	167.67	17880+1.0223i	2.77	0.0035	84.1
	500	1.14	188.12	31978+1.6079i	4.96	0.0045	139.3
4	200	4.10	288.43	2029.7+0.027514i	0.31	0.0018	38.8
	300	3.04	289.16	2741.0-0.33990i	0.43	0.0021	52.4
	400	1.89	291.82	4430.4+ 0.028942i	0.69	0.0026	84.1
	500	1.14	300.08	7461.8 – 0.25688i	1.16	0.0034	139.3
7	200	4.10	362.29	1164.3+ 0.17530i	0.18	0.0016	38.8
	300	3.04	362.89	1571.7 – 0.034318i	0.24	0.0018	52.4
	400	1.89	365.06	2536.3 + 0.23819i	0.39	0.0023	84.1
	500	1.14	371.58	4248.1- 0.10469i	0.66	0.0030	139.3

A resonance frequency is found when the imaginary part of the input impedance is zero, and the curve of this imaginary parts vs. frequency is rising before being zero. According to the results in Table 1, the first resonance frequency increases when the temperature of the CNT increases, and its value is also increased for a higher radius of the bundle. Table 1 includes both the relaxation time used for calculations depending on the temperatures of the CNT and the frequency $F_v = v/2\pi$ below which resonances seem to be suppressed. The relaxation frequency, and obviously F_v, both increase when the temperature increases. From the results, it is clear that the input impedance increases when the temperature of the CNT increases. However, its value is lower for the bundles than for the simple SWCNT nanoantenna. In Fig. 4, Figs. 4a and 4b show, respectively, the real and imaginary parts of the input impedance for the simple dipole nanoantenna ($l = 1$). Figs. 4c and 4d show the results for the SWCNT bundle dipole nanoantennas of one layer ($l = 4$), and Figs. 4e and 4f the results for two layers ($l = 7$). The temperature increase reduces the resonance peaks, as found in [19], but for a nanoantenna with SWCNT. Fig. 5 shows the magnitude of the current distributions for the simple ($l = 1$) dipole nanoantenna (Fig. 5a) and for the SWCNT bundle dipole nanoantennas of one ($l = 4$) and two layers ($l = 7$), Figs. 5b and 5c, respectively. The current distributions correspond to those for the first resonant frequencies and, as expected, a resonant half-wave sinusoid form is obtained for each case. Results show that, as much as for a simple SWCNT dipole nanoantenna as for a given bundle, the maximum amplitude of the current decreases when the temperature increases and, as a consequence, the input impedance increases. The larger the perimeter of the nanotube bundle, the higher the magnitude of the current. Results above may seem obvious; however, a brief analysis is pertinent. Fig. 6 shows the effective mean free length as a function of the absolute temperature resulting from the interaction of electrons in the CNT with defects and acoustic and optical phonons in a low electric field regimen.

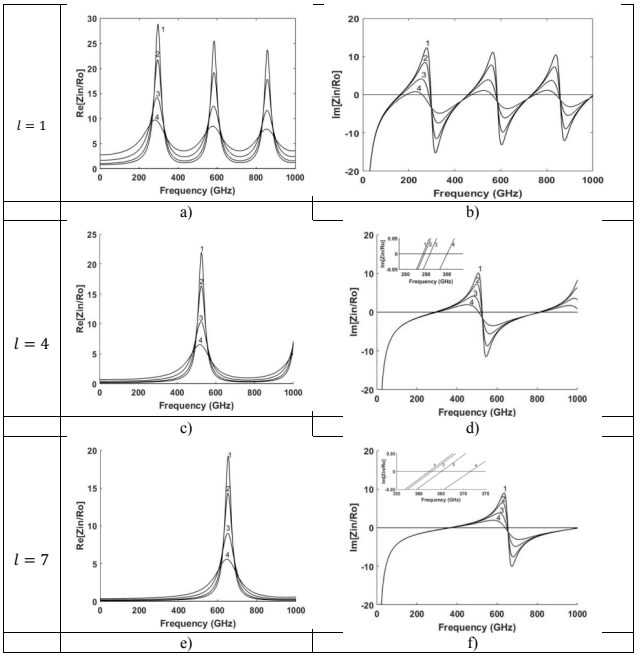

FIGURE 4. Normalized real and imaginary parts of the input impedance. Figs. 4a and 4b show, respectively, the real an imaginary parts of the input impedance for the simple dipole nanoantenna ($l = 1$). Figs. 4c and 4d show results for the SWCNT bundle dipole nanoantennas of one layer ($l = 4$), and Figs. 4e and 4f the results for two layers ($l = 7$). The nanoantenna has a total length of $2L = 20$ μm. Numbers 1, 2, 3 and 4 correspond to $T = 200, 300, 400$ and 500 K, respectively.

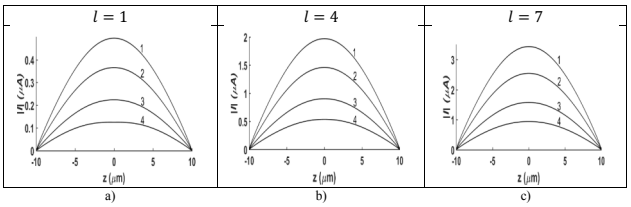

FIGURE 5. Magnitude of the current distribution corresponding to the first resonance frequencies according to Table 1. Fig. 5a shows the result for the simple ($l = 1$) dipole nanoantenna. Fig. 5b shows the result for the SWCNT bundle dipole nanoantennas of one ($l = 4$) layer, and Fig. 5c shows the result for two layers ($l = 7$). Numbers 1, 2, 3 and 4 correspond to results for $T = 200, 300, 400$ and 500 K, respectively.

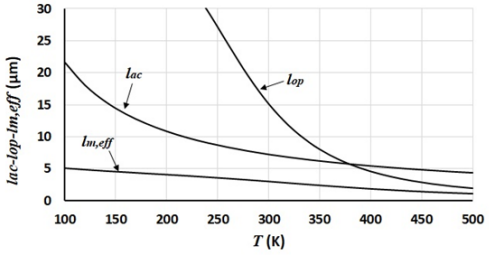

FIGURE 6. Mean free lengths, considering acoustic phonons, l_{ac}, optical phonons, l_{op}, and resulting effective mean free length considering scattering by defects and both acoustic and optical phonons, $l_{m,eff}$.

The mean free lengths, which consider only acoustic or optical phonons are also shown. According to these results, the interaction with optical phonons can start to be significant at temperatures not too high above room temperature, even in the regime of low applied field and low frequencies. In this case, the shorter mean free length resulting from interaction with optical phonons will prevail over the mean free length resulting from interaction with acoustic phonons. Therefore, the effective mean free path will be determined primarily by the optical phonons and is reduced with the consequent increase in the relaxation frequency. This, in turn, decreases the conductivity and the current, generating an increase in the input impedance. Now, well, an increase in the bundle diameter produces an increase in the current such that, for a fixed input voltage, a lower input impedance and an increase in the efficiency are obtained. Additionally, a higher temperature and a bundle diameter increase both produce an increase in the first resonance frequency. These characteristics may be attractive for the use of this type of nanoantennas in nanocircuits where low radiation efficiencies might not be a real inconvenience since their use would be restricted to very short distances. Previous experimental results [29] demonstrated the phenomena of plasmon resonance in SWCNTs and proved the antenna effect in SWCNTs in terahertz and far-infrared ranges. More experiments should be carried out to prove the performance of nanoantennas with bundles of SWCNTs. Some studies corroborated that, due to dispersion at surfaces and grain boundaries, resistivity increases significantly as the dimensions of copper traces are reduced. Besides, metallic wires may have reduced conductivity at high temperatures due to increased scattering of electrons and phonons. This higher resistivity leads to increased ohmic losses, which can dampen the resonant current oscillations in the antenna. This damping effect could shift the resonance frequency or broaden the resonance peak, resulting in less sharp and distinct resonances compared to CNT-based antennas [30], [31]. The higher resistivity might also affect the effective electrical length of the antenna. With increased resistivity, the penetration depth of the current into the metal wire decreases, effectively shortening the antenna's electrical length. This can lead to a higher resonance frequency than expected because the antenna would appear electrically shorter than its physical length. Although improved methods, such as electron beam lithography and atomic layer deposition, are now available for manufacturing nanometer-thick wires, the presence of impurities and defects can still significantly affect conductivity. Therefore, the choice of carbon nanotubes for nanoantenna manufacturing continues to be a visionary alternative not only for its conductivity properties, but for the mechanical and thermal properties that emerge at the nanoscale, justifying their potential use in nanoantennas and other advanced electronic devices in quantum technologies of computation, sensing, and communication [32]. Research on nanoantennas, particularly those based on carbon nanotubes, could also be relevant in manipulating and detecting quantum signals in biological systems, for example [33].

VI. CONCLUSION

In this work, the temperature dependence of the resonance properties of dipole antennas built by bundles of SWCNTs was investigated by considering the surface area of densely packed CNTs. A comparison was made between a simple SWCNT dipole nanoantenna and bundle dipole nanoantennas of one and two layers, but conclusions could be extrapolated to more layers. Hallén's equation was numerically solved by the method of moments considering the dynamic quantum mechanical conductivity for armchair CNTs with a corresponding relaxation frequency calculated from the Matthiessen formula, where the interaction of electrons in the nanotube with defects and acoustic and optical phonons is considered. In particular, the effects of the temperature on the first resonance frequency, the input impedance, and the efficiency were analyzed. An increase in the impedance was found as the temperature increased, however, the increase in the bundle diameter comparatively reduces the input impedance due to an increase in the current, which, in turn, could explain the increase in efficiency for each beam diameter when the temperature increases. Note that the efficiency is calculated at a different resonant frequency for each temperature in each case. The efficiency of CNT bundle nanoantennas depends on interrelated factors such as input impedance and high-frequency resistance, both influenced by temperature through conductivity and carrier scattering. This complexity makes it difficult to compare results between different studies, as the specific calculation conditions vary in the literature. Future work could focus on comparing the results obtained here with experimental to further validate their robustness.

APPENDIX: A SHORT NOTE ON POSSIBLE EXPERIMENTAL REALIZATIONS OF CNT BUNDLES

Fabricating bundles of carbon nanotubes (CNTs) in straight, long, and parallel configurations for dipole nanoantenna design involves several advanced techniques [34]-[37]. Among these techniques that stand out are Chemical Vapor Deposition (CVD) and Template-Based Growth. In the first of these techniques, controlling the growth conditions, such as temperature, gas flow rate, and catalyst composition, it is possible to grow CNTs that are straight, long, and aligned. In the second, a template with nanoscale channels or pores is used to guide the growth of CNTs. The template ensures that the CNTs grow in a parallel and aligned manner. Anodized aluminum oxide membranes are commonly used as templates. The catalyst is deposited into the pores of the template, and the CNTs grow within these confined spaces, resulting in aligned bundles. Post-growth alignment techniques could also be used to align and bundle CNTs. In the dielectrophoresis, for example, an electric field is applied to a solution containing CNTs, causing them to align along the field lines. In the magnetic field alignment, CNTs are functionalized with magnetic nanoparticles, and then aligned using a magnetic field. Finally, in Flow Alignment, CNTs in

a liquid suspension can be aligned by flowing the liquid through narrow channels or under shear flow conditions. Individual CNTs or small bundles can also be mechanically manipulated using tools such as atomic force microscopy (AFM) or scanning tunneling microscopy (STM). These methods allow for precise placement and alignment but are typically limited to small-scale production. Alternatively, an electrospinning procedure can be used, which involves an electric field to draw very fine fibers from a liquid containing CNTs. This method can produce long and continuous CNT fibers that are aligned due to the electric field applied during the spinning process. Finally, Self-Assembly Techniques could involve chemical or physical processes to guide the spontaneous organization of CNTs into aligned structures. For example, surfactants or polymers can induce CNT alignment through intermolecular interactions. Practical considerations and challenges are present in all of these techniques and methods. For example, ensuring high purity and low defect density in CNTs is crucial for their performance in nanoantennas. Besides, techniques need to be scalable for practical applications, which can be challenging for methods that require precise control at the nanoscale. Lastly, for practical device applications, integrating CNTs with other materials and ensuring good electrical contact is important. In this sense, analyzing the input impedance and resonance properties of feasible carbon nanotubes nanoantennas is always of significant importance.

REFERENCES

[1] A. S. C. Vakhrushev Alexander V., Kodolov Vladimir I., Haghi A. K., Ed., *Carbon Nanotubes and Nanoparticles: Current and Potential Applications*. Palm Bay, Florida, USA: Apple Academic Press Inc., 2019.

[2] A. Todri-Sanial, J. Dijon, and M. Antonio, Eds., *Carbon Nanotubes for Interconnects Process, Design and Applications*. Switzerland: Springer International Publishing, 2017.

[3] M. Hajjyahya, M. Ishtaiwi, J. Sayyed, and A. Saddouq, "Design of Carbon Nanotube Antenna in Nanoscale Range", *Open J. Antennas Propag.*, vol. 9, pp. 57–64, 2021, doi: 10.4236/ojapr.2021.94005.

[4] Y. N. Jurn, M. Abdulmalek, H. A. Rahim, S. A. Mahmood, and W. Liu, "Electromagnetic Modelling of Bundle of Single-walled Carbon Nanotubes with Circular Geometry for Antenna Applications", *ACES J.*, vol. 32, no. 6, pp. 531–541, 2017.

[5] E. Medina-Guerra and Á. Salazar, "Effect of the radius on the resonance properties of carbon nanotube dipole antennas", *J. Commun. Technol. Electron.*, vol. 62, no. 10, 2017, doi: 10.1134/S1064226917100096.

[6] M. Shou and R. Saito, "Surface plasmons in graphene and carbon nanotubes", *Carbon N. Y.*, vol. 167, 2020, doi: 10.1016/j.carbon.2020.05.019.

[7] R. R. Hartmann, J. Kono, and M. E. Portnoi, "Terahertz science and technology of carbon nanomaterials", *Nanotechnology*, vol. 322001, no. 25, pp. 1–16, 2014, doi: 10.1088/0957-4484/25/32/322001.

[8] Y. Wang, J. Shuo, M. Ming, and H. Chen, "Electromagnetic Radiation from Carbon Nanotube at Terahertz Frequency", *2012 5th Glob. Symp. Millim. Waves (GSMM 2012)*, pp. 554–558, 2012, doi: 10.1109/GSMM.2012.6314399.

[9] J. Hao and G. W. Hanson, "Infrared and Optical Properties of Carbon Nanotube Dipole Antennas", *IEEE Trans. Nanotechnol.*, vol. 5, no. 6, pp. 766–775, 2006, doi: 10.1109/TNANO.2006.883475.

[10] G. W. Hanson, "Fundamental Transmitting Properties of Carbon Nanotube Antennas", *IEEE Trans. Antennas Propag.*, vol. 53, no. 11, pp. 3426–3435, 2005, doi: 10.1109/TAP.2005.858865.

[11] M. F. Malek, Y. N. Jurn, S. A. Mahmood, and A. T. Maolood, "Performance Evaluation of the Electromagnetic Behavior of the Bundle SWCNTs with Circular Geometry", *2015 IEEE Int. Conf. Electron. Comput. Commun. Technol.*, pp. 1–6, 2015, doi: 10.1109/CONECCT.2015.7383893.

[12] Y. N. Jurn, M. F. Malek, W. Liu, and S. A. Mahmood, "An Investigation of Single-Walled Carbon Nanotubes Bundle Dipole Antenna at THz Frequencies", *2014 IEEE Int. Conf. Control Syst. Comput. Eng.*, 2014, doi: DOI:10.1109/ICCSCE.2014.7072782.

[13] S. Choi, S. Member, and K. Sarabandi, "Performance Assessment of Bundled Carbon Nanotube for Antenna Applications at Terahertz Frequencies and Higher", *IEEE Trans. Antennas Propag.*, vol. 59, no. 3, pp. 802–809, 2011, doi: 10.1109/TAP.2010.2103023.

[14] P. Franck, Dominique Baillargeat and Beng Kang Tay, "Trade - offs in Designing Antennas from Bundled Carbon Nanotubes", *2012 IEEE/MTT-S Int. Microw. Symp. Dig.*, pp. 6–8, 2012, doi: 10.1109/MWSYM.2012.6259507.

[15] Y. Huang, W. Yin, and Q. H. Liu, "Performance Prediction of Carbon Nanotube Bundle Dipole Antennas", *IEEE Trans. Nanotechnol.*, vol. 7, no. 3, pp. 331–337, 2008, doi: 10.1109/TNANO.2007.915017.

[16] K. Sarabandi and S. Choi, "Radiation Efficiency Assessment of Bundle Carbon Nanotubes Antenna at Terahertz Frequency Range", *2011 XXXth URSI Gen. Assem. Sci. Symp.*, 2011, doi: 10.1109/URSIGASS.2011.6050396.

[17] Y. Wang, Y. M. Wu, L. L. Zhuang, S. Q. Zhang, L. W. Li, and Q. Wu, "Electromagnetic Performance of Single Walled Carbon Nanotube Bundles", *2009 Asia Pacific Microw. Conf.*, pp. 190–193, 2009, doi: 10.1109/APMC.2009.5385406.

[18] J. J. Plombon; Kevin P. O'Brien, Florian Gstrein, Valery M. Dubin and Yang Jiao, "High-frequency electrical properties of individual and bundled carbon nanotubes High-frequency electrical properties of individual and bundled carbon nanotubes", *Appl. Phys. Lett.*, vol. 063106, pp. 21–24, 2007, doi: 10.1063/1.2437724.

[19] A. G. Chiariello, C. Forestiere, G. Miano, and A. Maffucci, "Scattering properties of carbon nanotubes", COMPEL: The International Journal for Computation and Mathematics in Electrical and Electronic Engineering, vol. 32, no. 6, pp. 1793–1808, 2013, doi: 10.1108/COMPEL-10-2012-0206.

[20] E. Pop, D. A. Mann, K. E. Goodson, and H. Dai, "Electrical and thermal transport in metallic single-wall carbon nanotubes on insulating substrates", *J. Appl. Phys.* 101, 093710 2007, doi: 10.1063/1.2717855.

[21] Orfanidis S.J., *Electromagnetic Waves and Antennas*. https://www.ece.rutgers.edu/~orfanidi/ewa/, 2016.

[22] A. Peigney, C. Laurent, E. Flahaut, R. R. Bacsa, and A. Rousset, "Specific Surface Area of Carbon Nanotubes and Bundles of Carbon Specific surface area of carbon nanotubes and bundles of carbon nanotubes", *Carbon N. Y.*, vol. 39, pp. 507–514, 2001, doi: 10.1016/S0008-6223(00)00155-X.

[23] S. A. Maksimenko, A. Lakhtakia, O. Yevtushenko, and A. V Gusakov, "Electrodynamics of carbon nanotubes: Dynamic conductivity, impedance boundary conditions, and surface wave propagation", *Phys. Rev. B*, vol. 60, no. 24, pp. 136–149,1999, doi.org/10.1103/PhysRevB.60.17136

[24] D. Akinwande and P. H.-S. Wong, *Carbon Nanotube and Graphene Device Physics*. New York, United States of America: Cambridge University Press, 2011.

[25] Walton C. Gibson, *The Method of Moments in Electromagnetics*, Third Edit. Taylor & Francis Group, LLC, 2022.

[26] Fikioris G. and Wu T., On the Application of Numerical Methods to Hallen's Equation, IEEE Trans. Antennas Propagat., 49, pp. 383-392, 2001, doi: 10.1109/8.918612.

[27] Fikioris G., Anastasios Papathanasopoulos, On the thin-wire integral equations for carbon nanotube antennas, IEEE Trans. Antennas Propagat., 66, Issue: 7, pp. 3567-3576, 2018, doi: 10.1109/TAP.2018.2826651.

[28] N. Fichtner, X. Zhou, and P. Russer, "Investigation of carbon nanotube antennas using thin wire integral equations", *Adv. Radio Sci*, vol. 6, pp. 209–211, 2008, doi: 10.5194/ars-6-209-2008.

[29] S. A. Maksimenko, M. V. Shuba, P.P. Kuzhir, G.Ya. Slepyan, "Antenna Resonances in Carbon Nanotubes: Theoretical Model and

Experimental Verification", Proceedings of the 15th IEEE International Conference on Nanotechnology, July 27-30, 2015, Rome, Italy, doi: 10.1109/NANO.2015.7388949.

[30] W. Wu; S. H. Brongersma; M. Van Hove; K. Maex, Influence of surface and grain-boundary scattering on the resistivity of copper in reduced dimensions, Appl. Phys. Lett. 84, 2838–2840 (2004), doi: 10.1063/1.1703844.

[31] Katayun Barmak; Tik Sun; R. Coffey, Impact of surface and grain boundary scattering on the resistivity of nanometric Cu interconnects, AIP Conf. Proc. 1300, 12–22 (2010), doi: 10.1063/1.3527118.

[32] Baydin, A.; Tay, F.; Fan, J.; Manjappa, M.; Gao,W.; Kono, J., Carbon Nanotube Devices for Quantum Technology. Materials 2022, 15, 1535. https://doi.org/10.3390/ma15041535.

[33] Cao et al., Quantum biology revisited, Sci. Adv. 2020; 6 : eaaz4888, doi: 10.1126/sciadv.aaz4888.

[34] E. Amram Bengio, Damir Senic, Lauren W. Taylor, Dmitri E. Tsentalovich, Peiyu Chen, Christopher L. Holloway, Aydin Babakhani, Christian J. Long, David R. Novotny, James C. Booth, Nathan D. Orloff, and Matteo Pasquali, High efficiency carbon nanotube thread antenas, Appl. Phys. Lett. 111, 163109 (2017), doi: 10.1063/1.4991822.

[35] Anderson, E. C., Cola, B. A., Photon-assisted tunneling in carbon nanotube optical rectennas: Characterization and modeling, ACS Appl. Electron. Mater. 2019, 1, 692– 700, doi.org/10.1021/acsaelm.9b00058.

[36] Lina Tizani, Yawar Abbas, Ahmed Mahdy Yassin, Baker Mohammad and Moh'd Rezeq, Single wall carbon nanotube based optical rectenna, RSC Adv., 2021,11, 24116-24124, doi: 10.1039/D1RA04186J.

[37] Zhifu Yin, Ao Ding, Hui Zhang and Wang Zhang, The Relevant Approaches for Aligning Carbon Nanotubes, Micromachines 2022, 13, 1863, doi: 10.3390/mi13111863.